

Theory of the phases and atomistic structure of yttria-doped zirconia

S. Ostanin,¹ E. Salamatov,² A. J. Craven,³ D. W. McComb,⁴ and D. Vlachos^{3,4}

¹*Department of Physics, University of Warwick, Coventry CV4 7AL, United Kingdom*

²*Physico-Technical Institute, Ural Branch of RAS, 426001 Izhevsk, Russia*

³*Department of Physics and Astronomy, University of Glasgow, Glasgow G12 8QQ, United Kingdom*

⁴*Department of Chemistry, University of Glasgow, Glasgow G12 8QQ, United Kingdom*

(Received 11 June 2002; published 28 October 2002)

Atomistic configurations of yttria-stabilized zirconia between 3 and 10 mol % Y_2O_3 were relaxed using the pseudopotential technique. The results showed a phase transition to the cubic (c) $(\text{ZrO}_2)_{100-x}(\text{Y}_2\text{O}_3)_x$ at $x \sim 10$ mol %. The electron-energy-loss near-edge spectra, calculated using the linear muffin-tin orbital method and relaxed defect geometry, agree with experiment. In the displacive limit of the double-well potential model, the vibration modes, corresponding to a soft phonon of c - ZrO_2 , were calculated for each composition of yttria-stabilized zirconia. The effect of anharmonicity yields the fine structure in the spectral density which is associated with stabilization at $x < 10$ mol %. In studying the phonon dynamics, we use the displacement probability density which quantifies accurately the transition temperature above which the c phase is stabilized.

DOI: 10.1103/PhysRevB.66.132105

PACS number(s): 61.72.Bb, 63.20.Ry, 63.70.+h

Pure ZrO_2 exhibits three polymorphs: the monoclinic (m) phase, with cations located in sevenfold coordination environments, the tetragonal (t) phase between 1170 and 2370 °C where Zr^{4+} is found in distorted eightfold coordination, and, finally, the high-temperature c phase whose eightfold cations are perfectly coordinated. Y_2O_3 has a large solid solubility range in ZrO_2 and can be used to stabilize the t phase of $(\text{ZrO}_2)_{100-x}(\text{Y}_2\text{O}_3)_x$ over the composition range $2 < x < 9$ mol % and the c phase with $4 < x < 40$ mol %. In yttria-stabilized zirconia (YSZ), the trivalent dopant Y^{3+} substitute for some of the host cations and, in order to maintain charge neutrality, one O vacancy must be created for each pair of dopant cations. The presence of relaxed vacancies (i) make the local atomic environments of YSZ rather different from the corresponding stoichiometric phases and (ii) reduces the average cation coordination number to a value between 7 and 8 depending on the dopant concentration.

The x-ray absorption findings¹ suggest that dopant cations do not take an active part in stabilization. If the vacancies associate with Zr ions, it may support a coordination-driven ordering model of stabilization. Placing Y in the next-nearest-neighbor (NNN) cation positions allows the coordination of Zr in the nearest-neighbor (NN) sites to the vacancy to be similar to the arrangement in the m phase while Y remains eightfold coordinated. The *ab initio* calculations of YSZ (Refs. 2 and 3) have reported that the NNN sites to the vacancy are favored for Y. Recent neutron diffraction experiments report⁴ that at low x there are vacancies arranged in pairs on the NN anion sites in the [111] fluorite direction, with the cation site between them occupied by the sixfold-coordinated Zr. Electrostatic considerations suggest that vacancies should repel. From this point of view, the divacancy configuration along $\langle 111 \rangle$ would be favored over those along $\langle 100 \rangle$ or $\langle 110 \rangle$. Because of the small size of Zr^{4+} , the electrostatic arguments place ZrO_2 on the border between the eightfold-coordinated fluorite and sixfold-coordinated structures.⁵ The presence of the larger Y, which possesses the longer Y-O bond compared to the Zr-O bond, appears to shift this balance in favor of sevenfold and sixfold

coordination for Zr resulting in the local m - and brookite-type³ coordination environments, respectively.

In doped ZrO_2 , no microscopic mechanism for the phase transitions has been proposed up to now. In pure ZrO_2 a zone-boundary soft phonon X_2^- , which breaks the c symmetry of the O sublattice, displacing anions toward their positions in the t phase, might be responsible for the $c \rightarrow t$ transformation. The displacements of O atoms lead to half of the Zr-O bonds becoming stronger and the other half weaker compared with the bonds in an ideal c phase. By calculating the c/a unit cell deformation and atomic displacements of O in the t phase Jansen⁶ showed that the c structure is unstable against the internal O displacements along the z direction. The height of this instability barrier depends strongly on the volume. The previous calculations of the X_2^- -phonon frequency within the harmonic approximation^{7,8} yield an imaginary frequency of 5.2–5.5 THz. This simply indicates that the c - ZrO_2 is unstable at low temperatures. At high temperatures the effects of anharmonicity might stabilize the c phase. In YSZ, the experimental data⁹ are not fully clarified for this soft mode because of the static disorder in the O sublattice. Thus, a theoretical investigation of this vibration mode would be useful. We believe that allowance for anharmonicity can give a criterion to the microscopic mechanism of stability. The frozen-phonon method and self-consistent phonon approximation were used to calculate the phonon frequency and its temperature dependence, respectively.

Model. To relax the positions of atoms in the $(96-y)$ -atom YSZ supercells ($y=1,2,3$) the plane-wave, pseudopotential-based free energy molecular dynamics technique¹⁰ is used. That allows $(\text{ZrO}_2)_{100-x}(\text{Y}_2\text{O}_3)_x$ to be modeled between 3 and 10 mol % Y_2O_3 . In the 95-atom cell, which corresponds to $x=3.2$ mol %, the effect of starting the static optimization with O in the t geometry reduces the total energy by ~ 1 eV/cell relative to the same c configuration relaxed. The vacancy strongly prefers Y in NN sites before relaxation but, after relaxation, a configuration with two Y NNN shows the lowest energy. The 94- and 93-atom cells

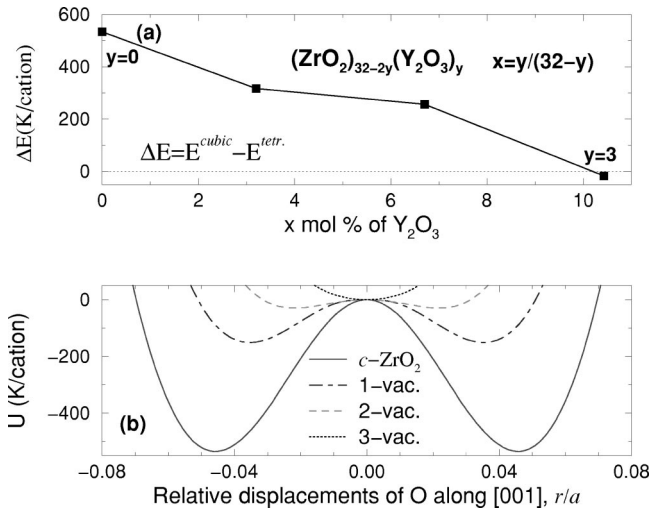


FIG. 1. Difference in the relaxed energy between the t and c configurations of YSZ is shown in panel (a). In panel (b), a decay of the double-well potential U with Y_2O_3 doping is shown as the change in energy plotted vs the t displacements of the O sublattice for each concentration of Y_2O_3 . The U 's were shifted to the common zero energy at $r=0$.

model 6.7 and 10.4 mol % YSZ. In the lowest-energy configuration of the divacancy cell, the vacancies are along the fluorite [111] direction and separated by the sixfold-coordinated Zr.

Figure 1, in panel (a), shows the difference in energy between the most stable c and t configurations. The energy difference is given in Kelvin per cation to relate it an equivalent temperature change. In the mono- and divacancy cells, the t configurations are more stable while, for trivacancies, the c configuration is marginally more stable. Experimentally, the same change in stability is observed. Electron-energy-loss near-edge structure (ELNES) of YSZ has been measured¹¹ demonstrating the features of the experimental O K -edge shapes which depend on the crystal structures and the Y_2O_3 composition. Using the relaxed configurations of YSZ, the agreement between experiment and theory has been improved significantly³ compared to that using the pure ZrO_2 structures.¹² Hence, our theoretical modeling can reflect the realities of relaxation.

Within the frozen-phonon method, the effective phonon potential is the difference in energy between perfect and distorted lattices for various amplitudes of atomic displacements made according to the symmetry of the phonon. Figure 1, in panel (b), displays the effective potential U , calculated as a function of the O t displacements, r/a , along the z axis. The relative temperature units used give an idea of the temperature changes. In the trivacancy YSZ cell, U has a single minimum at $r=0$. With decreasing the Y_2O_3 content, U develops two minima; i.e., its form becomes similar to that of the X_2^- phonon in ZrO_2 . In pure ZrO_2 , the energy difference $\Delta E^{c-t} = 0.046$ eV/ ZrO_2 is in a good agreement with experimental value¹³ of 0.057 eV/ ZrO_2 derived from enthalpy differences at corresponding phase transition temperatures. In fact, the depth and position of the $U(r/a)$ minimum for pure ZrO_2 are in very good agreement with previous

calculations.^{6,8} The small differences between these theoretical results are due to using different equilibrium volumes.

The modified pseudoharmonic approximation, developed to calculate the low-frequency anharmonic defect dynamics,¹⁴ has been applied recently to study the structural instabilities of Zr.^{15,16} In the one-phonon inelastic neutron scattering spectrum, the position and width of the peak determine the phonon frequency and lifetime, respectively. The corresponding intensity is calculated as the imaginary part of the one-phonon Green's function¹⁷ $g_q(\omega, T) = (1/\pi)\Gamma(\omega_q, T)/\{[\omega - \tilde{\omega}_q(T)]^2 + \Gamma^2(\omega_q, T)\}$, where $\tilde{\omega}_q(T)$ is the renormalized frequency and $\Gamma(\omega_q, T)$ appears due to scattering. At high temperatures the phonon linewidth depends weakly on the attenuation. The defect-dependent attenuation $\Gamma(\omega, E) = A_x \omega(E)$ ($A_x = 0.1, 0.15, 0.2, 0.25$) is used for each $y=0,1,2,3$ concentration of Y_2O_3 . Thus, the coefficient A_x increases linearly with increasing the dopant concentration while its values were obtained using the calculated results of well-defined harmonic modes of YSZ compared to available experimental data.⁹ To calculate ω , $U(r/a)$ was approximated by an eighth-degree polynomial.¹⁶ The variable E , introduced with the equilibrium distribution function $\rho(E) = \exp(-E/T)/T$, shows the characteristic time of variation, $\tau_E \sim 1/\Gamma \gg 1/\omega_q$, which allows calculation of the frequency for each E within the pseudoharmonic approximation.

The results can be summarized as follows: at all temperatures, one can find (i) the basic (b) vibrations localized near minima of U , with the frequencies ω_b close to the principal frequency ω_0 [$m\omega_0^2 = \partial^2 U(r)/\partial r^2|_{r=r_{min}}$], and (ii) the excited (e) overbarrier vibrations with $\omega_e \approx \omega_0/2$. With increasing temperature, the portion of the b vibrations, $c_b = 1 - \exp(-E_c/T)$ (E_c is the local-transition energy), diminishes while $c_e = 1 - c_b$ increases and, hence, new harmonics arise. The b peak moves towards the low-frequency range while the e peak shows the opposite trend. These findings are in qualitative agreement with previous numerical results.¹⁸ In pure ZrO_2 , the calculated ω_e of ~ 10 THz is a reasonable value when compared to the acoustic-phonon branches observed at this point of the Brillouin zone.⁹ At room temperature, the $g_q(\omega)$ of pure ZrO_2 plotted in panel (a) of Fig. 2 shows the b peak only. With increasing temperature, the intensity of the b peak falls and the cubic-like e vibrations become dominant at $T=3000$ K. Figure 2, in panel (b), shows the evolution of $g_q(\omega)$ with increasing Y_2O_3 at $T=1000$ K. In c - ZrO_2 , the b vibrations are dominant at this intermediate temperature whereas both types of vibrations may coexist in YSZ at low concentrations of Y_2O_3 . Figure 1(b) shows that U of c - ZrO_2 has minima with a high barrier between them giving rise to distinct frequencies for the two modes, as seen in Fig. 2(a). As seen in Fig. 2(b), introducing three vacancies into the cell gives a single minimum in U leading to only a b mode whose frequency is lower than the ω_b of c - ZrO_2 . In the mono- and divacancy cases, the U barriers lower so that the e and b modes merge into an unresolved low-frequency structure.

Since the arbitrary parameter Γ is used to calculate g_q , it would be desirable to consider the displacement proba-

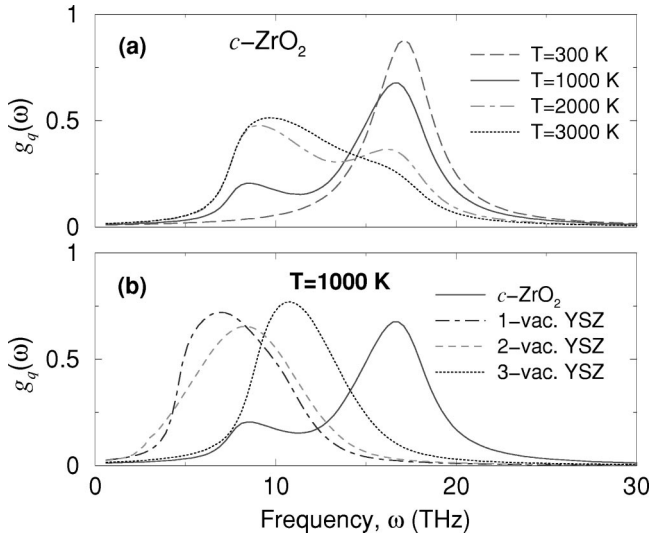


FIG. 2. Spectrum of the soft phonon mode in pure c -ZrO₂ at different temperatures, plotted in panel (a), and its changes in YSZ with yttria doping, which are shown in panel (b) for 1000 K.

bility density (DPD),¹⁹ which is free from Γ : $P(r) = \pi^{-0.5} \int dE \rho(E) \sqrt{\beta(E)} e^{-[r-r_0(E)]^2 \beta(E)}$, where $\beta = (m\omega^2)/(2k_B E)$ and r_0 is $\langle r \rangle$ at E . In the case of a single-well harmonic potential at $r=0$, $P_{r=0}(T)$ decreases gradually with increasing temperature. Consequently, an increase of the zero-coordinate DPD can indicate the stabilization process for the high-symmetry phase.

Figure 3, in panel (a), shows the DPD's of YSZ at room temperature. In pure ZrO₂ and the monovacancy cell, there is a peak associated with the b mode. This may illustrate the room-temperature instability of the c configuration. The T dependence of the DPD's at $r=0$ is shown in panel (b) of Fig. 3. At $r=0$ in the di- and trivacancy YSZ cells, the $\log_{10}P$ vs $\log_{10}T$ plots are almost linearly decreasing. In pure ZrO₂ and the monovacancy cell, $\log_{10}P$ initially rises and then, with increasing temperature, the linearly decreasing behavior appears again. In ZrO₂, the linearly decreasing behavior starts at ~ 2500 K i.e., close to the t - c transition temperature observed, whereas, in the monovacancy case, the linearly decreasing behavior starts around room temperature. The upper boundary of the single t -phase field in the experi-

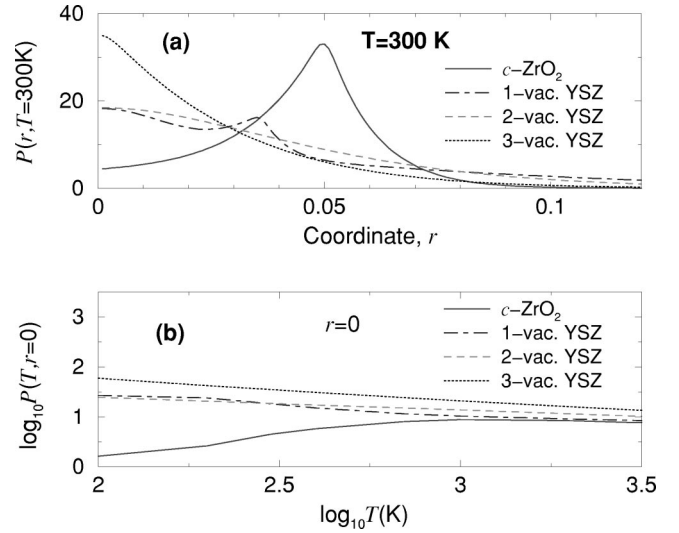


FIG. 3. The displacement probability densities $P(T,r)$: the room-temperature P 's ranging between 0 and 10 mol % Y₂O₃, which are plotted in panel (a), and the zero-coordinate P 's, shown in panel (b).

mental phase diagram shows a similar rapid drop of temperature with Y₂O₃ concentration, suggesting that the onset of the linear decrease of $\log_{10}P$ with $\log_{10}T$ marks the limit of the stability of the t phase.²⁰

According to our present knowledge, it is not possible to give a more detailed explanation whether a change in the slope of the DPD's can quantify the stabilization process. Any appropriate integral function might be calculated. Since the t - c transition temperature, estimated from the maximum point of $P_{r=0}(T)$, correlates with the experimental findings of YSZ, we suggest to use this DPD integral function as a quantitative criterion of stability. It would be worthwhile to apply this guess to other zirconia containing materials.

In summary, the calculated DPD features of YSZ are in very good agreement with experiment, suggesting that the zero-coordinate DPD, $P_{r=0}(T)$, can be used as a criterion of stability. This report might be considered as a first attempt to get some insight into whether the t - and c -phases can coexist in YSZ.

The authors wish to thank Mike Finnis, Ali Alavi, and Tony Paxton for stimulating discussions.

¹P. Li, I. Chen Wei, and J.E. Penner-Hahn, Phys. Rev. B **48**, 10 063 (1993); **48**, 10 082 (1993).

²G. Stapper, M. Bernasconi, N. Nicoloso, and M. Parrinello, Phys. Rev. B **59**, 797 (1999).

³S. Ostanin, A.J. Craven, D.W. McComb, D. Vlachos, A. Alavi, A.T. Paxton, and M.W. Finnis, Phys. Rev. B **65**, 224109 (2002).

⁴J.P. Goff, W. Hayes, S. Hull, M.T. Hutchings, and K.N. Clausen, Phys. Rev. B **59**, 14 202 (1999).

⁵M.W. Finnis, A.T. Paxton, M. Methfessel, and M. van Schilfgaarde, Phys. Rev. Lett. **81**, 5149 (1998).

⁶H.J.F. Jansen, Phys. Rev. B **43**, 7267 (1991).

⁷F. Detraux, P. Ghosez, and X. Gonze, Phys. Rev. Lett. **81**, 3297 (1998).

⁸S. Fabris, A.T. Paxton, and M.W. Finnis, Phys. Rev. B **63**, 094101 (2001).

⁹D.W. Liu, C.H. Perry, A.A. Feinberg, and R. Currat, Phys. Rev. B **36**, 9212 (1987); D.N. Argyriou and M.M. Elcombe, J. Phys. Chem. Solids **57**, 343 (1996).

¹⁰A. Alavi, J. Kohanoff, M. Parrinello, and D. Frenkel, Phys. Rev. Lett. **73**, 2599 (1994).

¹¹D. Vlachos, A.J. Craven, and D.W. McComb, J. Phys.: Condens. Matter **13**, 10 799 (2001).

- ¹²S. Ostanin, A.J. Craven, D.W. McComb, D. Vlachos, A. Alavi, M.W. Finnis, and A.T. Paxton, *Phys. Rev. B* **62**, 14 728 (2000).
- ¹³R. Ackermann, E.G. Rauh, and C.A. Alexander, *High. Temp. Sci.* **7**, 304 (1975).
- ¹⁴E.I. Salamatov, *Phys. Status Solidi B* **197**, 323 (1996); **177**, 75 (1993).
- ¹⁵S.A. Ostanin, E.I. Salamatov, and V.Yu. Trubitsin, *Phys. Rev. B* **58**, R15 962 (1998).
- ¹⁶S.A. Ostanin, E.I. Salamatov, and V.Yu. Trubitsin, *Phys. Rev. B* **57**, 5002 (1998).
- ¹⁷A.A. Maradudin and A.E. Fein, *Phys. Rev.* **128**, 2589 (1962).
- ¹⁸Yu.N. Gornostyrev, M.I. Katsnelson, A.V. Trefilov, and S.V. Tret'jakov, *Phys. Rev. B* **54**, 3286 (1996); C.A. Condat and P.W. Lamberti, *ibid.* **53**, 8354 (1996).
- ¹⁹S. Aubry, *J. Chem. Phys.* **62**, 3217 (1975).
- ²⁰R.A. Miller *et al.*, in *Science and Technology of Zirconia*, edited by A.H. Heuer and L.W. Hobbs, *Advances in Ceramics*, Vol. 3 (American Ceramic Society, OH, 1981).